remaining crystals were suspended in $CHCl_3$. The solution was filtered, the volume of $CHCl_3$ was reduced under a stream of Ar, and the crystals were allowed to form under vapor diffusion conditions in the freezer using Et_2O as the equilibrating solvent. The vapor diffusion recrystallization was repeated to afford the complex as orange-red crystals, mp 208-215 °C. Anal. Calcd for $C_{24}H_{36}ClFeN_2NaO_8$: C, 48.46; H, 6.10; N, 4.71. Found: C, 48.42; H, 6.09; N, 4.68. The thin, needle-shaped crystals were mounted in thin-walled glass capillaries prior to X-ray diffraction analysis. The crystal belongs to the *Pbcn* space group, with maximum dimensions of 0.10 × 0.10 × 0.20 mm, the cell dimensions were a = 10.833 (Å), b = 17.167(3) Å, c = 14.718(2) Å, V = 2737 Å^3, D_c = 1.45 g/cm^3, ν_c = 1.8 cm^{-1}, molecules/unit cell = 4, λ = MoKα; total number of reflections collected and observed were 2621 and 962, respectively, R = 0.052, R_w = 0.052. All nonhydrogen atoms were treated with anisotropic thermal parameters. The hydrogen atoms were placed in geometry-fixed positions and were not refined. The weighting scheme was based upon unit weights. A final difference electron density map displayed no unaccounted electron density.

c. **Cryptand 2·Ag$^+$.** The $AgClO_4$ complex of **2** was prepared by simultaneously mixing acetone solutions containing equivalent amounts of **2** and salt. The solvent was evaporated under reduced pressure; the residue was dissolved in $CHCl_3$ and then filtered. The solvent was reduced (Ar stream) to 0.5 mL. Two vapor diffusion crystallizations (0.5 mL of $CHCl_3$/4 mL of Et_2O) afforded the complex as orange plates (mp 209-210 °C). Small, thin plates of the compound were mounted in thin-walled glass capillaries prior to X-ray diffraction analysis. Details of the procedure have been given previously.[29] The maximum crystal dimensions were 0.05 × 0.10 × 2.0 mm. The space group is $P2_1/n$, the cell constants were a = 17.186(2) Å, b = 9.152(1) Å, c = 17.802(1) Å, β = 108.93(1)°, V = 2649 Å^3, molecules/unit cell = 4, D_c = 1.71 g/cm^3, μ = 1.5 cm^{-1}, λ = MoKα, reflections collected = 5121, reflections observed = 1900, R = 0.056, R_w = 0.061. The structure was solved using SHELX-86. All nonhydrogen atoms were treated with anisotropic thermal parameters. The hydrogen atoms were placed in geometry-fixed positions and were not refined. A final difference electron density map displayed no unaccounted electron density.

Acknowledgment. We thank the National Institute of Health (to G.W.G., GM 36262) and the National Science Foundation (to A.K. CHE 9000531) for grants that supported this work.

Supplementary Material Available: FAB/MS spectra of **1**·Ag$^+$, **2**·Ag$^+$, and **6**·Ag$^+$ and figure of equilibrium concentration of the **2**·Na$^+$ complex as the potential is scanned across the $E^{\circ\prime}$ value of the **2**$^+$/**2** couple (5 pages). Ordering information is given on any current masthead page.

(29) Holton, J.; Lappert, M. F.; Ballard, D. G. H.; Pearce, R.; Atwood, J. L.; Hunter, W. E. *J. Chem. Soc., Dalton Trans.* **1979**, 45.

Dissociative Electron Transfer. New Tests of the Theory in the Electrochemical and Homogeneous Reduction of Alkyl Halides

Jean-Michel Savéant

Contribution from the Laboratoire d'Electrochimie Moléculaire de l'Université de Paris 7, Unité Associée au CNRS No. 438, 2 place Jussieu, 75251 Paris Cedex 05, France.
Received May 26, 1992

Abstract: In the testing of the theory of dissociative electron transfer with experimental data pertaining to the electrochemical and homogeneous reduction of alkyl halides, uncertainties arising from the estimation of the effect of solvent dynamics and reorganisation as well as of the resonance energy in the transition state are minimized by a comparative strategy which utilizes information derived from outer-sphere electron-transfer data gathered in the same solvent. Application of this strategy leads to a good agreement between theory and experiment in the electrochemical case. In the homogeneous case, the agreement is equally satisfactory in the case of tertiary halides. With the less sterically hindered secondary and primary halides, the reaction possesses an S_N2 character involving small bonded interactions in the transition state in accord with previous stereochemical results and reaction entropy determinations.

As shown earlier,[1] important assumptions underlying the Marcus-Hush model[2] of outer-sphere electron-transfer dynamics are not applicable to dissociative electron transfer. In the latter type of reaction, electron transfer from an electrode or from an outer-sphere homogeneous electron donor, D$^{\bullet-}$, to the acceptor molecule, RX, is concerted with the breaking of the R-X bond:

$$\text{electrochemical: } RX + e^- \rightleftarrows R^\bullet + X^-$$

$$\text{homogeneous: } RX + D^{\bullet-} \rightleftarrows R^\bullet + X^- + D$$

Representation of the potential energy by the R-X Morse curve in the reactant system and by a purely dissociative curve identical to the repulsive part of the R-X curve in the R$^\bullet$ + X$^-$ system and treatment of solvent reorganization in the Marcus-Hush fashion lead to a quadratic activation-driving force relationship:[1]

$$\Delta G^\ddagger = w_R + \Delta G_0^\ddagger\left(1 + \frac{\Delta G^\circ - w_R + w_P}{4\Delta G_0^\ddagger}\right)^2 \qquad (1)$$

(ΔG° is the standard free energy of the reaction, i.e., the opposite of the driving force in terms of free energy; $\Delta G_0^\ddagger$ is the standard activation free energy, i.e., the activation free energy of the forward and reverse reactions at zero driving force or, in other words, the intrinsic barrier free energy; w_R is the work required for bringing the reactants from infinity to reacting distance, i.e., to form the "precursor complex"; w_P is the work required to form the "successor complex", from infinity to reacting distance) where the intrinsic barrier $\Delta G_0^\ddagger$ is, neglecting the possible internal changes besides bond breaking (or assuming they are included in the Morse curve description), the sum of two terms:

(1) (a) Savéant, J.-M. *J. Am. Chem. Soc.* **1987**, *109*, 6788. (b) Savéant, J.-M. *Adv. Phys. Org. Chem.* **1990**, *26*, 1.

(2) (a) Marcus, R. A. *J. Chem. Phys.* **1956**, *24*, 4966. (b) Hush, N. S. *J. Chem. Phys.* **1958**, *28*, 962. (c) Marcus, R. A. Theory and Applications of Electron Transfers at Electrodes and in Solution. *Special Topics in Electrochemistry*; Rock, P. A., Ed.; Elsevier: New York, 1977; pp 161-179. (d) Marcus, R. A. *Faraday Discuss. Chem. Soc.* **1982**, *74*, 7. (e) Marcus, R. A.; Sutin, N. *Biophys. Biochim. Acta* **1985**, *811*, 265.

0002-7863/92/1514-10595$03.00/0

$$\Delta G_0^{\ddagger} = \frac{D_{RX} + \lambda_0}{4} \quad (2)$$

where D_{RX} is the R–X bond dissociation energy and λ_0 the Marcus–Hush solvent reorganization factor.

Alkyl halides, such as butyl and benzyl halides, have been taken as model compounds for the testing of the model[1a,3] because thermochemical data are available for these compounds, allowing the estimation of the driving forces and of the bond dissociation energies. In these tests of the theory, $\Delta G^{\ddagger}$ was derived from the experimental electrochemical or homogeneous rate data using, as pre-exponential factor, the heterogeneous or bimolecular frequencies, similarly to what was done in the original version of Marcus theory of outer-sphere electron transfer:[2a-c]

$$k = Z \exp\left(-\frac{\Delta G^{\ddagger}}{RT}\right) \quad (3)$$

with

$$Z^{el} = \left(\frac{RT}{2\pi M}\right)^{1/2} \quad (4)$$

(M: molar mass), in the electrochemical case, and

$$Z^{hom} = (a_1 + a_2)^2\left(\frac{8\pi RT}{\mu}\right)^{1/2} \quad (5)$$

(μ is the reduced molar mass of the two reactants; a_1 and a_2 are the hard-sphere equivalent radii of the two reactants), in the homogeneous case.

In fact, the identification of the pre-exponential factor with the collision frequency is certainly a crude approximation, and the same effects that have been shown to interfere in the case of outer-sphere electron transfers[4] should be taken into account here, namely the equilibrium constant for the formation of the precursor complex, the possible involvement of solvent relaxation in the control of the effective nuclear frequency for crossing the activation barrier, and, in the case of adiabatic processes, the avoided crossing energy in the estimation of the activation barrier (the avoided crossing energy should be subtracted from the activation energy derived from the simple crossing of the diabatic potential energy curves).

One purpose of the following discussion was to evaluate the impact of these factors on the experimental testing of the theory with data pertaining to the electrochemical and homogeneous reduction of alkyl halides. It will be shown that a comparative strategy utilizing available kinetic data for simple outer-sphere reactions in combination with the data pertaining to the dissociative electron-transfer reactions of interest in the same solvent leads to satisfactory results. Two additional points will be discussed, namely the use of the symmetry factor as a mechanistic diagnostical tool and the outer-sphere vs inner-sphere (S_N2) character of aromatic anion radical electron donors in their reaction with alkyl halides.

Results and Discussion

Improvement of the Model. Strategies for Comparison with Experimental Data. Similarly to the case of outer-sphere electron transfer, eqs 3–5 may be replaced by[4a,b]

$$k = K_A \kappa_e \nu_n \exp\left(-\frac{\Delta G^{\ddagger}}{RT}\right) \quad (6)$$

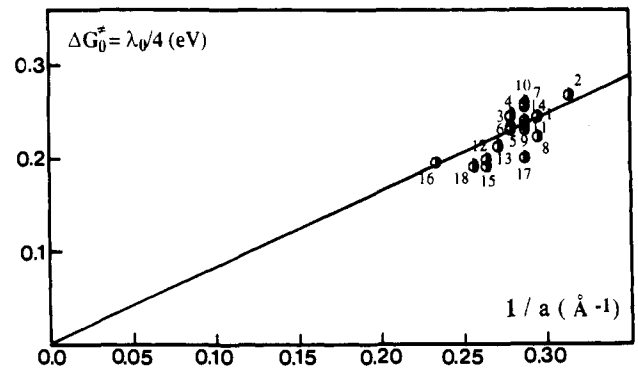

Figure 1. Electrochemical standard activation free energies of the reduction of aromatic molecules in *N,N'*-dimethylformamide as a function of their equivalent hard-sphere radius a: 1, benzonitrile; 2, 4-cyanopyridine; 3, *o*-tolunitrile; 4, *m*-tolunitrile; 5, *p*-tolunitrile; 6, phthalonitrile; 7, terephthalonitrile; 8, nitrobenzene; 9, *m*-dinitrobenzene; 10, *p*-dinitrobenzene; 11, *m*-nitrobenzonitrile; 12, dibenzofuran; 13, dibenzothiophene; 14, *p*-naphthoquinone; 15, anthracene; 16, perylene; 17, naphthalene; 18, *trans*-stilbene.

where K_A is the equilibrium constant for the formation of the precursor complex, ν_n is the effective nuclear frequency, and κ_e is the electronic transmission factor that includes the possible nonadiabaticity effects as a function of the electronic coupling matrix element. The latter energy (i.e., the resonance or avoided crossing energy) should also be subtracted from the values of $\Delta G^{\ddagger}$ that are derived from the diabatic potential free energy surfaces along the above-described procedure.

The effective nuclear frequency is expected to be dominated by the intramolecular vibration frequencies, here by the vibration frequency of the cleaving bond, that are generally larger than those of the solvent modes. Under such conditions, the dynamics of solvent fluctuations is expected to be the main factor that governs the effective value of the pre-exponential factor. Equation 6 should then be replaced by eq 7

$$k = K_A \kappa_e \nu \exp\left(-\frac{\Delta G^{\ddagger}}{RT}\right) \quad (7)$$

where ν can be expressed in the framework of a steady-state approximation, as[4d]

$$\frac{1}{\nu} = \frac{1}{\nu_i} + \tau_L \mathcal{F}\left(\frac{D_{RX} + \lambda_i}{D_{RX} + \lambda_i + 2\lambda_0}, \frac{\Delta G^{\ddagger}}{RT}\right) \quad (8)$$

where ν_i is the dominating intramolecular vibration frequency and τ_L the solvent longitudinal relaxation time. Equation 8 applies for both outer-sphere (with $D_{RX} = 0$) and dissociative ($\lambda_i = 0$ in the case where intramolecular changes besides bonding breaking are either negligible or integrated in the Morse curve approximation) electron transfers. From available numerical computations of the function $\mathcal{F}$,[4d-f] it appears that there is an approximate mutual compensation between the effects of $(D_{RX} + \lambda_i)/\lambda_0$ and of $\Delta G^{\ddagger}/RT$ on the values of the function $\mathcal{F}$. The magnitude of $\mathcal{F}$ (on the order of 1[4e]) and the values of τ_L (10^{-12} s^{-1} for DMF[5a-c]) and ν_i (on the order of 2.10^{13} s^{-1} in the butyl halide series[5d]) are such that the second term in eq 8 predominates over the first.

It follows that, for adiabatic ($\kappa_e = 1$) outer-sphere and dissociative electron transfers, the ratio of the pre-exponential factors should be approximately equal to the ratio of the two K_A constants if the avoided crossing energies are small and approximately the same in both cases. This observation points to a comparative strategy for testing the predictions of the theoretical model with the experimental data: instead of attempting an uncertain absolute

(3) Andrieux, C. P.; Le Gorande, A.; Savéant, J.-M. *J. Am. Chem. Soc.*, in press.

(4) (a) Sutin, N. Theory of Electron Transfer Reactions: Insights and Hinsights. *Progress in Inorganic Chemistry*; Lippard, S. J., Ed.; Wiley: New York, 1983; Vol. 30, pp 441–447. (b) Newton, M. D.; Sutin, N. *Annu. Rev. Phys. Chem.* **1984**, *35*, 437. (c) Sumi, H.; Marcus, R. A. *J. Chem. Phys.* **1986**, *84*, 4272. (d) Sumi, H.; Marcus, R. A. *J. Chem. Phys.* **1986**, *84*, 4894. (e) Sumi, H.; Marcus, R. A. *J. Electroanal. Chem.* **1986**, *204*, 59. (f) Nadler, W.; Marcus, R. A. *J. Chem. Phys.* **1987**, *86*, 3906. (g) Jortner, J.; Bixon, M. *J. Chem. Phys.* **1988**, *88*, 167. (h) Weaver, M.; McMannis, G. E. *Acc. Chem. Res.* **1990**, *23*, 294. (i) Grampp, G.; Jänicke, W. *Ber. Bunsen-Ges. Phys. Chem.* **1991**, *95*, 904. (j) Fawcett, W. R.; Blum, L. *Chem. Phys. Lett.* **1991**, *187*, 173.

(5) (a) Bass, S. J.; Nathan, W. I.; Meighan, R. M.; Cole, R. H. *J. Phys. Chem.* **1964**, *68*, 509. (b) Behret, H.; Schmidthals, F.; Barthel, J. *Z. Phys. Chem.* (Munich) **1975**, *96*, 73. (c) Barthel, J.; Bachhuber, K.; Buchner, R.; Gill, J. B.; Kleebaner, M. *Chem. Phys. Lett.* **1990**, *167*, 62. (d) Bellamy, L. J. *The Infrared Spectra of Complex Molecules*; Chapman and Hall: London, 1975, p 368.

Table I. Cyclic Voltammetric Reductive Cleavage of Butyl Bromides and Iodides:[a] Comparison between the Predictions of the Theory of Dissociative Electron Transfer and the Experimental Data

	Butyl Iodides						Butyl Bromides					
	n-BuI		*s*-BuI		*t*-BuI		*n*-BuBr		*s*-BuBr		*t*-BuBr	
$-E_m{}^b$	2.25_2		1.98_2		1.83_9		2.75_6		2.54_0		2.39_7	
$-\phi_r{}^b$	0.09_0		0.08_4		0.08_1		0.10_2		0.09_7		0.09_0	
A^{el} ($cm \cdot s^{-1}$)	4.5×10^4								5.1×10^4			
$\Delta G^{\ddagger}{}^{c,d}$	0.41_0		0.41_5		0.41_5		0.42_0		0.42_0		0.42_0	
$\Delta G^{\circ}{}_{RX/R^{\bullet}}{}^d$	0	0.11_2	0	0.11_2	0	0.11_2	0	0.12_1	0	0.12_1	0	0.12_1
$-E^{\circ}{}^b$	1.07_5	1.20_9	0.94_6	1.08_0	0.82_6	0.96_0	1.10_9	1.23_0	1.04_9	1.19_0	0.92_9	1.05_0
$\Delta G_0{}^{\ddagger}(exp^{al})^a$	0.87_5	0.82_3	0.82_3	0.77_0	0.81_5	0.76_2	1.05_1	1.00_6	0.99_5	0.94_2	0.98_9	0.94_4
$a_{RX}{}^e$	3.56		3.58		3.62		3.50		3.50		3.54	
a^e	3.04		3.05		3.06		2.82		2.82		2.83	
$\lambda_0{}^d$	1.03_6		1.03_2		1.02_9		1.11_7		1.11_7		1.11_3	
$D_{RX}{}^{d,f}$	2.56	2.67	2.38	2.49	2.20	2.31	3.00	3.12	2.95	3.07	2.87	2.99
$\Delta G_0{}^{\ddagger}(theor)^d$	0.90_0	0.92_7	0.85_3	0.88_0	0.80_7	0.83_5	1.02_9	1.05_9	1.01_7	1.04_7	0.99_6	1.02_6
α(pred)	0.34	0.36	0.36	0.37	0.36	0.37	0.32	0.32	0.32	0.33	0.33	0.32
α(theor)	0.35	0.37	0.36	0.38	0.36	0.38	0.31	0.33	0.33	0.35	0.33	0.35
$\alpha(exp^{al})$	0.30		0.33		0.32		0.25		0.25		0.20	

[a] In DMF + 0.1 M *n*-Bu_4NBF_4, at a glassy carbon electrode at 25 °C; scan rate = 0.1 V/s from the data in ref 8. [b] In V vs SCE. [c] $D = 10^{-5}$ $cm^2 \cdot s^{-1}$. [d] In eV. [e] In Å. [f] From literature thermochemical data (see text).

estimation of the parameters that govern the pre-exponential factor, the injection of experimental data pertaining to outer-sphere organic couples gathered in the same solvent into the treatment of the dissociative electron-transfer data of interest should minimize the impact of these uncertainties. In this connection, an extended set of experimental data is available for the electrochemical and homogeneous self-exchange reduction of a large variety of aromatic and heteroaromatic molecules in DMF,[6a,b] in which solvent reorganization is the dominant factor in the activation barrier.[6c] The same strategy also allows one to minimize similarly unavoidable uncertainties in the determination of the solvent reorganization factor λ_0 and of the resonance energy at the transition state.

Electrochemical Reduction of Alkyl Halides. Figure 1 shows the variation of the standard free energy of activation for the reversible reduction of a series of aromatic and heteroaromatic hydrocarbons in DMF with the inverse of their hard-sphere radii a, derived from previous results of Kojima and Bard.[6a] Instead of using the heterogeneous collision frequency, Z^{el} (eq 4) for extracting $\Delta G_0{}^{\ddagger}$ from the rate data, we plotted them against $1/a$ according to Hush's approximation:

$$\lambda_0 = 4\Delta G_0{}^{\ddagger} = e_0{}^2\left(\frac{1}{D_{op}} - \frac{1}{D_S}\right)\frac{1}{2a} \tag{9}$$

(e_0 is the electron charge; D_{op} and D_S are the dynamic and static dielectric constants of the solvent, respectively), which looks more consistent with the experimental results than Marcus's approximation in the present case. The intercept of the log k vs $1/a$ original data provides the average value of the pre-exponential factor, A^{el} in the series ($A^{el} = 5.1 \times 10^4$ $cm \cdot s^{-1}$) which will replace Z^{el} in eq 3 in the following treatments. The ensuing variations of $\Delta G_0{}^{\ddagger}$ with $1/a$ are represented in Figure 1. It then follows that

$$\lambda_0 \text{ (eV)} = \frac{3.15}{a \text{ (Å)}} \tag{10}$$

λ_0 for the reduction of the alkyl halides is obtained from this relationship after estimation of the hard-sphere radius of the RX molecule. In previous analyses,[1a] a was taken as the half-sum of the hard-sphere radii of RX, a_{RX}, and X, a_X. A better approximation appears to be[3]

$$a = \frac{a_X(2a_{RX} - a_X)}{a_{RX}} \tag{11}$$

The value of A^{el} is taken as equal to 5.1×10^4 $cm \cdot s^{-1}$, corrected by the square root of the ratio of the molar masses (eq 4) when required.

The comparison between the predictions of the dissociative electron-transfer theory and the experimental data is summarized in Tables I and II. The value of the intrinsic barrier free energy derived from the experimental data (namely the cyclic voltammetric peak potential, E_p, or the midpoint between the peak and the half-peak potential, E_m), $\Delta G_0{}^{\ddagger}(exp^{al})$, is compared to the value obtained from eq 2, $\Delta G_0{}^{\ddagger}$(theor). For obtaining $\Delta G_0{}^{\ddagger}(exp^{al})$, we apply eq 1 under a form suited to electrochemical reactions:

$$\Delta G^{\ddagger} = \Delta G_0{}^{\ddagger}\left[1 + \frac{E_{p,m} - (E^{\circ} + \phi_r)}{4\Delta G_0{}^{\ddagger}}\right]^2 \tag{12}$$

in which $E_{p,m}$ designates E_p or E_m according to the case, E°, the standard potential of the $RX + e^- \rightleftarrows R^{\bullet} + X^-$ couple, and ϕ_r, the potential difference between the reacting site and the solution. The reacting site is generally assumed to be located in the outer Helmoltz plane of the electrochemical double layer,[6b] and ϕ_r is obtained from previous measurements carried out in the same solvent (DMF) with the same supporting electrolyte cation (*n*-$Bu_4{}^+$).[6a] In the potential region of interest, the variation of ϕ_r with the electrode potential E is, with a good precision, linear. In volts

$$\phi_r = 0.011E - 0.052 \tag{13}$$

$\Delta G^{\ddagger}$, the activation free energy of the forward reaction, has two slightly different values, $\Delta G_m{}^{\ddagger}$ and $\Delta G_p{}^{\ddagger}$ according to whether it is derived from E_m or E_p, respectively:

$$\Delta G_m{}^{\ddagger} = \frac{RT}{F}\ln\left[A^{el}\left(\frac{RT}{\alpha F v D}\right)^{1/2}\right] + 0.145\frac{RT}{F} \tag{14}$$

$$\Delta G_p{}^{\ddagger} = \frac{RT}{F}\ln\left[A^{el}\left(\frac{RT}{\alpha F v D}\right)^{1/2}\right] - 0.780\frac{RT}{F} \tag{15}$$

where D is the diffusion coefficient of RX, v, the scan rate, and α, the transfer coefficient. In the establishment of eqs 14 and 15, the quadratic character of the activation–driving force relationship and thus the variation of the transfer coefficient with the electrode potential were neglected.[1a,7] Such a simplification is perfectly legitimate for each scan rate individually, since the potential difference between the foot and the peak of each individual voltammogram is small. In the derivation of $\Delta G_{m,p}{}^{\ddagger}$, α is obtained from the experimental data or, better, from predicted

(6) (a) Kojima, H.; Bard, A. *J. Am. Chem. Soc.* **1975**, *97*, 6317. (b) Delahay, P. *Double Layer and Electrode Kinetics*; Wiley: New York, 1965. (c) In the following analyses, the internal reorganization energy of these aromatic molecules is neglected vis à vis the solvent reorganization energy.

(7) (a) Lexa, D.; Savéant, J.-M.; Su, K. B.; Wang, D. L. *J. Am. Chem. Soc.* **1987**, *109*, 6464. (b) Andrieux, C. P.; Savéant, J.-M. *J. Electroanal. Chem.* **1989**, *267*, 15. (c) Lexa, D.; Savéant, J.-M.; Schäfer, H. J.; Su, K. B.; Vering, B.; Wang, D. L. *J. Am. Chem. Soc.* **1990**, *112*, 271.

Table II. Comparison between the Predictions of the Theory of Dissociative Electron Transfer and the Experimental Data for the Cyclic Voltammetric Reductive Cleavage of Benzyl Chloride and Bromide[a]

		$PhCH_2Cl$		$PhCH_2Br$	
E_p[b]	0.1 V·s^{-1}	−2.21		−1.71	
	1.0 V·s^{-1}	−2.30		−1.82	
	10.0 V·s^{-1}	−2.41		−1.94	
σ_r[b]	0.1 V·s^{-1}	-0.08_9		-0.07_8	
	1.0 V·s^{-1}	-0.09_1		-0.08_0	
	10.0 V·s^{-1}	-0.09_4		-0.08_2	
A^{el} (cm·s^{-1})		5.5×10^4		4.7×10^4	
$\Delta G^{\ddagger}$[c,d]	0.1 V·s^{-1}	0.39_9		0.39_4	
	1.0 V·s^{-1}	0.37_0		0.36_5	
	10.0 V·s^{-1}	0.34_1		0.33_7	
$\Delta G°_{RX/R\cdot}$[d]		0	0.11_2	0	0.12_1
$E°$[b]		-0.76_0	-0.87_2	-0.63_5	-0.75_6
$\Delta G_0^{\ddagger}(exp^{al})$[d]	0.1 V·s^{-1}	0.95_8	0.91_6	-0.81_6	-0.76_9
	1.0 V·s^{-1}	0.95_7	0.91_6	0.82_5	0.77_9
	10.0 V·s^{-1}	0.96_3	-0.92_3	0.83_6	0.79_2
	Av	0.96_0	0.91_9	0.82_6	0.78_0
a_X, a_{RX}, a;[e] λ_0[d]		1.81, 3.58, 2.70;	1.16_6	1.96, 3.61, 2.86;	1.10_1
D_{RX}[d,f]		2.99	3.10	2.30	2.42
$\Delta G_0^{\ddagger}(theor) = (D + \lambda_0)/4$[d]		1.03_9	1.06_7	0.85_0	0.88_0
α(pred)	0.1 V·s^{-1}	0.32_2	0.33_0	0.34_7	0.35_8
	1.0 V·s^{-1}	0.31_1	0.31_8	0.33_3	0.34_2
	10.0 V·s^{-1}	0.29_8	0.30_4	0.31_7	0.32_6
	Av	0.29_7	0.31_7	0.33_2	0.34_2
α(theor)	0.1 V·s^{-1}	0.33_6	0.35_4	0.35	0.37_6
	1.0 V·s^{-1}	0.32_6	0.34_3	0.33_7	0.36_0
	10.0 V·s^{-1}	0.31_3	0.33_1	0.32_0	0.34_4
	Av	0.32_5	0.34_3	0.33_7	0.36_0
$\alpha(exp^{al})$[g]	0.1 V·s^{-1}	0.30_8		0.34_1	
	1.0 V·s^{-1}	0.31_8		0.34_1	
	10.0 V·s^{-1}	0.28_1		0.29_8	
	Av	0.30_4		0.31_5	

[a] In DMF + 0.1 M n-Bu_4NBF_4, at a glassy carbon electrode at 25 °C from the data in ref 3. [b] In V vs SCE. [c] $D = 10^{-5}$ cm^2·s^{-1}. [d] In eV. [e] In Å. [f] From literature thermochemical data (see text). [g] The α value at each scan rate is derived from $E_{p/2} - E_p$, and the average also contains the value derived from $\partial E_p/\partial \log v$.

values as defined later on and $\Delta G_{m,p}^{\ddagger}$ thus computed along a rapidly converging iterative procedure. Once $\Delta G_{m,p}^{\ddagger}$ is known, $\Delta G_0^{\ddagger}(exp^{al})$ is obtained from eq 12 as

$$\Delta G_0^{\ddagger}(exp^{al}) = \{[(E_{m,p} - E° - \phi_r - 2\Delta G_{m,p}^{\ddagger})^2 - (E_{m,p} - E° - \phi_r)^2]^{1/2} - (E_{m,p} - E° - \phi_r - 2\Delta G_{m,p}^{\ddagger})\}/4 \quad (16)$$

In this estimation, $E°$ is calculated from literature thermochemical data with attention to the particular electrode reference used (here the aqueous saturated calomel electrode):

$$E° = \mu_{RX}^* - \mu_{R\cdot}^* - \mu_{X^-}^*$$

(the μ^*s are the standard chemical potentials of the subscript compounds). While $\mu_{X^-}°$ is available for solvents currently used in electrochemistry (here DMF), μ_{RX}^* and $\mu_{R\cdot}^*$ are only available in the gas phase. In the passage from the gas phase to the solvent, one may assume that the variation of μ_{RX}^* and $\mu_{R\cdot}^*$ are about the same (the solvation free energy of the permanent and induced R–X dipole would be nearly the same as that of the induced R· dipole).[7a,c,8] A first estimate of $E°$ is thus obtained from the μ_{RX}^* and $\mu_{R\cdot}^*$ gas-phase literature values and from the solvation free energy of X^-.[9] Another approach involves the following approximations.[8,10] The variation of μ_{RX}^* and $\mu_{R\cdot}^*$ would be the same as that of CH_3X and CH_4, respectively, independently of the nature of the polar solvent considered. A second estimate of $E°$ is thus obtained from the same thermochemical data[9a] and the known solvation free energies of CH_3X and CH_4 in water.[10] The second values are thus negative to the first by 0.134, 0.121, and 0.112 V for I, Br, and Cl, respectively.[8] When estimating the value of the bond dissociation energy to be used in the application of eq 2, the gas-phase value of the formation enthalpy of X· is used in all cases. In the case where $E°$ is estimated from the gas-phase values of $\mu_{RX}°$ and $\mu_{R\cdot}°$, D_{RX} is accordingly calculated from the gas-phase formation enthalpies of RX and R·. In the case where the difference in the solvation free energies of RX and R· is approximated by the difference between CH_3X and CH_4, the same amount is added to the gas-phase value of D_{RX}.

Perusal of the results displayed in Tables I and II shows that the theoretically predicted intrinsic barriers are in quite good agreement with the experimental data when $E°$ and D_{RX} are estimated on the basis of RX and R· gas-phase data. The agreement is not as good with the second estimation of $E°$ and RX.

The good accord between theoretical expectations and experimental data may, at first sight, seem to critically rely on the initial analysis of the rate data pertaining to aromatic anion radicals from which A^{el} and λ_0 were estimated. This is in fact not the case. Even large deviations from the values we have selected do not lead, provided they are properly correlated according to the Kojima and Bard data, to dramatically different results. An overestimation of A^{el} indeed leads to a correlated underestimation of λ_0 and vice versa. This is, for example, illustrated by the fact that previous treatments based on collision frequencies[1a,3] and utilizing also Kojima and Bard's data led to a not much less satisfactory adherence between theory and experiment.

(8) Andrieux, C. P.; Gallardo, I.; Savéant, J.-M.; Su, K. B. *J. Am. Chem. Soc.* **1986**, *108*, 638.

(9) (a) Cox, B. G.; Hedvig, G. R.; Parker, A. J.; Watts, D. W. *Aust. J. Chem.* **1974**, *27*, 477. (b) Geske, D. H.; Ragle, M. A.; Bambeneck, J. L.; Balch, A. L. *J. Am. Chem. Soc.* **1964**, *86*, 987. (c) Benson, S. W. *Thermodynamical Kinetics*, 2nd ed.; Wiley: New York, 1976. (d) Wagman, D. D.; Evans, W. H.; Parker, V. B.; Schumm, R. H.; Halow, I.; Bailey, S. M.; Churney, K. L.; Nuttal, R. L. *J. Phys. Chem. Ref. Data* **1982**, *11*, Suppl. 2.

(10) (a) Hush, N. S. Z. *Electrochemistry* **1957**, *61*, 734. (b) Eberson, L. *Acta Chem. Scand.* **1982**, *B36*, 533.

Another aspect of the dissociative electron-transfer theory can be tested using the same experimental data, namely the quadratic character of the activation–driving force relationship upon comparing the experimental values of the transfer coefficient $\alpha(\text{exp}^{al})$ with the predicted, α(pred), and theoretical, α(theor), values. α(pred) is the value obtained from eq 17, taking for $\Delta G_0^{\ddagger}$ the

$$\alpha = \frac{1}{2}\left(1 + \frac{E_{p,m} - E^\circ - \phi_r}{4\Delta G_0^{\ddagger}}\right) \qquad (17)$$

experimental value, $\Delta G_0^{\ddagger}(\text{exp}^{al})$, obtained from the experimental E_m or E_p data by means of eq 16, whereas α(theor) is obtained from eq 17 using for $\Delta G_0^{\ddagger}$ the theoretical value derived from eq 2 as just explained above. It is seen from Tables I and II that, although the experimental values of α are somewhat smaller than predicted, the striking fact that they lie well below 0.5 is nicely explained by the quadratic character of the activation–driving force relationship, taking into account that the reduction potential is in all cases much more negative than the standard potential of the $RX + e^- \rightarrow R^\bullet + X^-$ reaction.

A more direct test of the variation of the transfer coefficient with the driving force would be to examine its possible variation with the scan rate in cyclic voltammetry. Such experiments[8] have indeed shown that such a trend exists. However the variation of α with the driving force is detected with less precision than in the case of outer-sphere electron transfer (see refs 2b and 11 and references cited therein), because of the necessity of using as electrode glassy carbon instead of mercury which limits the range of scan rates in which meaningful experiments can be carried out. The detected variations are therefore not as distinctly beyond the experimental uncertainty as in the case of outer-sphere electron-transfer reactions.

Table II shows the results obtained along the same lines of an even more detailed investigation of benzyl chloride and bromide in DMF,[12] where several scan rates instead of one in the preceding case were used. We see that there is a good agreement between the predictions of the theory and the experimental values of the intrinsic barrier. The agreement is again better when potentials and the bond dissociation energies are estimated directly from literature RX and R$^\bullet$ gas-phase data than when the second procedure ($\Delta G_{RX/R^\bullet} \neq 0$) is used. The same is true for the values of the transfer coefficient. We see in Table II that there is a definite trend, in the case of benzyl halides, for the value of α to decrease upon raising the scan rate, and consequently the driving force, as predicted by the theory. This provides good evidence for the quadratic character of the activation–driving force relationship in spite of the fact that the theoretical and predicted values of α are somewhat larger than the experimental values.

Homogeneous Reduction of Alkyl Halides by Aromatic Anion Radicals. The same strategy as in the electrochemical case was followed here for determining the homogeneous pre-exponential factor, A^{hom}, and the solvent reorganization factor, λ_0^{hom}, using the Kojima and Bard[6a] data for the homogeneous self-exchange electron-transfer reactions of the same series of aromatic and heteroaromatic molecules in DMF. A straight line having the slope predicted by the Marcus model was fit to the original log k vs $1/a$ data. The intercept then provided the average value of A^{hom} (= 5.1×10^{12} M^{-1} s^{-1} [12]). Figure 2 shows the resulting variations of the intrinsic barrier free energy as a function of the inverse of the hard-sphere radius. λ_0 for the reaction of the

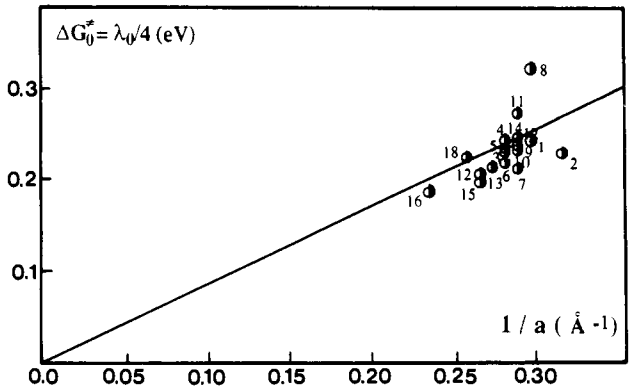

Figure 2. Homogeneous self-exchange standard activation free energies of the reduction of aromatic hydrocarbons in *N,N'*-dimethylformamide as a function of their equivalent hard-sphere radii, *a*: 1, benzonitrile; 2, 4-cyanopyridine; 3, *o*-tolunitrile; 4, *m*-tolunitrile; 5, *p*-tolunitrile; 6, phthalonitrile; 7, terephthalonitrile; 8, nitrobenzene; 9, *m*-dinitrobenzene; 10, *p*-dinitrobenzene; 11, *m*-nitrobenzonitrile; 12, dibenzofuran; 13, dibenzothiophene; 14, *p*-naphthoquinone; 15, anthracene; 16, perylene; 17, naphthalene; 18, *trans*-stilbene.

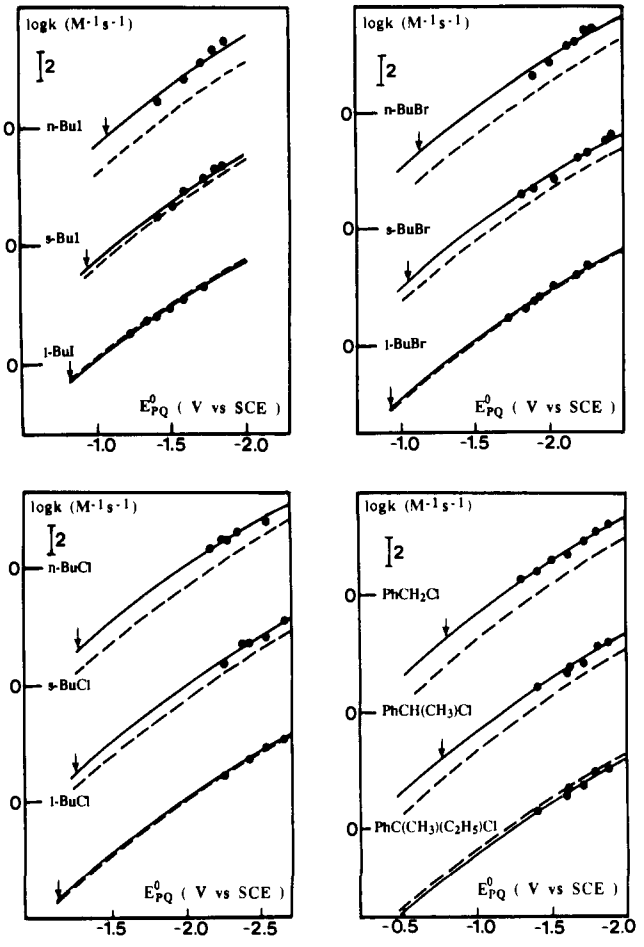

Figure 3. Variations of the rate constant of the reaction of aromatic anion radicals with alkyl halides (in DMF + 0.1 M n-Bu_4BF_4) with the standard potential of the mediator couple: ●, experimental points; ↓, location of the standard potential of the $RX/R^\bullet + X^-$ couple. Full lines are best fits according to eq 1. Dashed lines are theoretical predictions.

(11) Savéant, J.-M.; Tessier, D. *Faraday Discuss. Chem. Soc.* **1982**, *74*, 57.

(12) (a) Such a value of the pre-exponential factor appears consistent with the predictions of eq 7, since, with κ_e being assumed equal to 1, $\tau_L \simeq 10^{-12}$ s, $\mathcal{F} \simeq 1$, and $K_A \simeq 0.4$ and with a resonance energy of ca. 1 kcal/mol, a reasonable value of self-exchange electron transfer in aromatic anion radicals results from recent quantum mechanical calculations.[4i] (b) Significantly higher values of the resonance energy (2.5–6 kcal/mol) have been recently estimated,[12c] leading to the contention that aromatic anion radicals would react in an inner-sphere rather than outer-sphere fashion with their parents and with alkyl halides. These estimations are in fact based on several questionable assumptions and analyses. One series of estimations was indeed obtained from the strict application of the Marcus equation, giving λ_0 and making use of a pre-exponential factor assumed to be equal to the bimolecular collision frequency (itself taken rather arbitrarily to be equal to 10^{11} $M^{-1}\cdot s^{-1}$). The other was derived from the comparison of electrochemical and homogeneous rate data under the assumptions that there is no resonance energy in the electrochemical reactions of interest (yet considered as adiabatic processes), that the pre-exponential factors in both cases are equal to the collision frequencies (taken as equal to 10^4 $cm\cdot s^{-1}$ and 10^{11} $M^{-1}\cdot s^{-1}$, respectively), and that, for estimating the electrochemical λ_0, the Marcus rather than the Hush relationship applies. (c) Eberson, L.; Shaik, S. S. *J. Am. Chem. Soc.* **1990**, *112*, 4484.

Table III. Comparison between the Predictions of the Theory of Homogeneous Dissociative Electron Transfer and the Experimental Rate Data[a] for the Reaction of Butyl Halides[b] and Benzyl Chlorides[c]

compound	$-E^\circ$ (V vs SCE)	a_{RX} (Å)	a (Å)	λ_0^{hom} (eV)	D_{RX} (eV)	$\Delta G_0^\ddagger$ (eV) theor	$\Delta G_0^\ddagger$ (eV) exp[al]
n-BuI	1.07_5	3.56	3.04	1.01_0	2.5_6	0.89_2	0.77_2
s-BuI[d]	0.94_6	3.58	3.04	1.00_9	2.3_8	0.75_8	0.73_6
t-BuI[d]	0.82_6	3.62	3.06	1.00_6	2.2_0	0.71_2	0.72_1
n-BuBr	1.10_9	3.50	2.82	1.06_1	3.0_0	1.01_5	0.90_6
s-BuBr[d]	1.04_9	3.50	2.82	1.06_1	2.9_5	1.00_3	0.94_0
t-BuBr[d]	0.92_9	3.54	2.83	1.06_1	2.8_7	0.98_3	0.98_2
n-BuCl	1.26_7	3.45	2.67	1.10_3	3.5_0	1.15_1	1.06_8
s-BuCl[d]	1.25_8	3.47	2.68	1.10_0	3.4_5	1.13_8	1.07_7
t-BuCl[d]	1.13_8	3.51	2.69	1.09_7	3.4_2	1.12_9	1.12_0
$PhCH_2Cl$	0.76_0	3.58	2.70	1.09_3	2.9_9	1.02_1	0.92_5
$PhCH(CH_3)Cl$	0.75_1	3.71	2.73	1.08_6	2.9_4	1.00_6	0.93_6
$PhC(CH_3)C_2H_5)Cl$	0.63_1	3.84	2.77	1.07_5	2.9_1	0.99_6	1.01_1

[a] In DMF + 0.1 M n-Bu_4BF_4 at 20 °C unless otherwise stated. [b] From ref 5. [c] From ref 13. [d] 10 °C.

aromatic anion radicals, Q, with the alkyl halides, RX, was then derived from

$$\lambda_0^{hom}\ (eV) = 3.32\left(\frac{1}{a_Q} + \frac{1}{a} - \frac{2}{a_Q + a}\right) \qquad (18)$$

(the hard-sphere radii are expressed in Å), where the slope is that of the straight line in Figure 2.

Analysis of the experimental data for the butyl halides[8] and for benzyl chloride,[13] displayed in Figure 3 under the form of log $k - E_{PQ}^\circ$ (E_{PQ}°: the standard potential of the electron donor couple P/Q. k: rate constant of the reaction $RX + Q \rightarrow R^\bullet + X^- + P$) plots, was carried out according to the following procedure. The driving force of the reaction was obtained from

$$\Delta G^\circ = E_{PQ}^\circ - E^\circ \qquad (19)$$

Since, in the electrochemical case, the values of E°, the standard potential of the $RX/R^\bullet + X^-$ couple, derived under the assumption that $\Delta G_{RX/R^\bullet}^\circ$ is negligible, lead to the best fit with the experimental data, we have selected the same values for the present analysis. A value of $\Delta G_0^\ddagger$ is then derived from eq 1 (with $w_R = w_P = 0$) for each electron donor by means of

$$\Delta G_0^\ddagger = \frac{[(\Delta G^\circ - 2\Delta G^\ddagger)^2 - (\Delta G^\circ)^2]^{1/2} - (\Delta G^\circ - 2\Delta G^\ddagger)}{4} \qquad (20)$$

where, $\Delta G^\ddagger$, the activation free energy, is derived from the rate constant k according to

$$\Delta G^\ddagger\ (eV) = \frac{RT}{F} \ln\left(\frac{A^{hom}}{k}\right) \qquad (21)$$

The mean value of $\Delta G_0^\ddagger$ over the whole series of electron donors is reported for each halide in Table III under the heading $\Delta G_0^\ddagger(exp^{al})$ and was used to draw the full lines shown in Figure 3 using eqs 1 and 21. The satisfactory fit of this line with experimental rate data indicates the applicability of the activation–driving force relationship (1) for all compounds.

The values of $\Delta G_0^\ddagger(exp^{al})$ may now be compared with the theoretical values derived from

$$\Delta G_0^\ddagger = \frac{\lambda_0^{hom} + D_{RX}}{4} \qquad (22)$$

where λ_0^{hom} is estimated from eq 18 and D_{RX} obtained from the gas-phase thermochemical data as in the electrochemical case.

Overall, there is a satisfactory agreement between the experimental and theoretical values of $\Delta G_0^\ddagger$, as seen in Table III and in Figure 3, where the ensuing reconstructed log $k - E_{PQ}^\circ$ theoretical plots are represented as dashed lines.

It is clearly seen that the theory predicts quite correctly the differences observed upon changing the halogen atom from I to Br and Cl, at the level both of the intrinsic barriers and of the slopes of the activation–driving force plots.

It however distinctly appears that, given the halogen and changing the nature of the reacting carbon, the agreement is better for the tertiary halides than for the secondary and primary halides. This trend clearly appears even when account is taken of the fact that the uncertainties in the thermochemical data and in the values of λ_0 and of the pre-exponential factor may affect the observed differences between $\Delta G_0^\ddagger(exp^{al})$ and $\Delta G_0^\ddagger$(theor). From the mere fact that tertiary alkyl radicals are more stable than secondary and primary alkyl radicals, it is expected that D_{RX} increases in this series and E° becomes less and less negative. We thus expect both $\Delta G_0^\ddagger$(theor) and $\Delta G_0^\ddagger(exp^{al})$ to become larger and larger from tertiary to secondary and primary. This is what is observed for $\Delta G_0^\ddagger$(theor), but the trend is opposite for $\Delta G_0^\ddagger(exp^{al})$. Thus, taking the theory–experiment agreement as good for the tertiary halides, it is seen that the theory overestimates the intrinsic barrier in the case of secondary and primary halides even though the difference remains small (ca. 100 meV at maximum).

These observations suggest that, in the absence of strong steric hindrance, the transition state would be stabilized, albeit by a small amount, vis-ã-vis the transition state predicted for a dissociative electron transfer from an outer-sphere electron donor. The question thus arises whether this stabilization would involve bonded interactions. In favor of a positive answer is the previous finding that, when reacting optically active 2-octyl iodide, bromide, or chloride with anthracene anion radical, although racemization prevails, a small but significant amount of inversion (on the order of 10%) is observed.[14] It may thus be envisaged that the outer-sphere dissociative electron transfer between the anion radical and the alkyl halide occurs along two competitive pathways, the outer-sphere dissociative electron transfer that would lead to racemization and an S_N2-type substitution leading to inversion (Scheme I).

However with stabilization energies of the transition state on the order of 50–100 meV as found here, resulting in an acceleration of the reaction of one to two orders of magnitude, one would expect a much larger ratio of inversion over racemization. It follows that a dissociation of the radical resulting from the S_N2 substitution into the aromatic hydrocarbon and the alkyl radical should also be envisaged. Thus, in the absence of strong steric hindrance, the main initial step would be an S_N2 substitution leading to a radical that would undergo a partial, though possibly preponderant, dissociation into the aromatic hydrocarbon and the alkyl radical in which the stereochemical integrity of the reacting carbon would be lost.

One consequence of the instability of the S_N2 substitution radical vis-ã-vis the products of the outer-sphere dissociative electron transfer is that there is no driving force advantage of the former over the latter. One is thus led to conclude that the partially bonded transition state of the S_N2 pathway is stabilized vis-ã-vis that of the outer-sphere electron transfer pathway by

(13) Lund, T.; Lund, H. *Acta Chem. Scand. B* **1987**, *41*, 93.

(14) Hebert, E.; Mazaleyrat, J. P.; Nadjo, L.; Savéant, J.-M.; Welvart, Z. *Nouv. J. Chim.* **1985**, *9*, 75.

means of resonance between the two mesomeric structures:

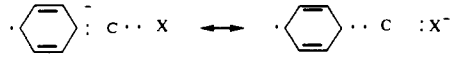

to an extent able to overrun the slight driving force disadvantage and the fact that the entropy of the S_N2 transition state is expected to be smaller than that of the outer-sphere dissociative electron-transfer transition state.

This latter point has been recently confirmed experimentally.[15] The variations of the rate constant with temperature were indeed found to be different for *n*-BuBr as compared to *t*-BuBr and other sterically hindered alkyl bromides. Although the present level of experimental accuracy actually appears as insufficient to detect the small change in slopes of Arrhenius plots that the competition between the ET and S_N2 pathway would predict,[15a] both series of experiments indicate that the average activation entropies are smaller with the primary bromide than with sterically hindered bromides (by ca. 10 eu).[16]

There is thus convergent kinetic (comparison of the activation–driving force plots, temperature dependence studies) and stereochemical evidence that, in the absence of strong steric hindrance, the reaction of aromatic anion radicals follows, with a slight kinetic preference, an S_N2 rather than an outer-sphere dissociative ET pathway even though most of the stereochemical integrity of the reacting carbon is ultimately lost. The kinetic preference is however small and does not support seriously in practice the qualms recently expressed[15b] as to the use of aromatic anion radicals as standards for an outer-sphere dissociative electron-transfer behavior in the investigation of the mechanism by which other nucleophiles (electron donors) react with primary halides. In this connection, the method of the "kinetic advantage" consists in locating the point corresponding to an unknown electron donor in the activation–driving force plot constructed from a series of aromatic anion radicals. The S_N2 character of the reaction of an unknown electron donor is then derived from the observation that its representative point is located significantly above the aromatic anion radical line. This approach was first proposed and applied in the case of electrochemically generated iron(I) and cobalt(I) porphyrins[17] and further applied to organic nucleophiles[18a–c] and to other low-valent metalloporphyrins.[15a] For nucleophiles that react with a primary or secondary halide faster than an aromatic anion radical of same standard potential, such as unemcumbered iron(I) or cobalt(I) porphyrins, it can be concluded a fortiori that an inner-sphere mechanism is followed. The ambiguity will only affect the cases where the unknown electron donor point is located in the close vicinity of the aromatic anion radical line. As an example, it may be noted that sterically encumbered iron(I) porphyrins are located slightly below the line.[15a] At any rate, it should be emphasized that when the representative point is located in the close vicinity of the aromatic anion radical line, the S_N2 character of the initial step does not necessarily imply the stereoselectivity of the overall reaction.

Scheme I

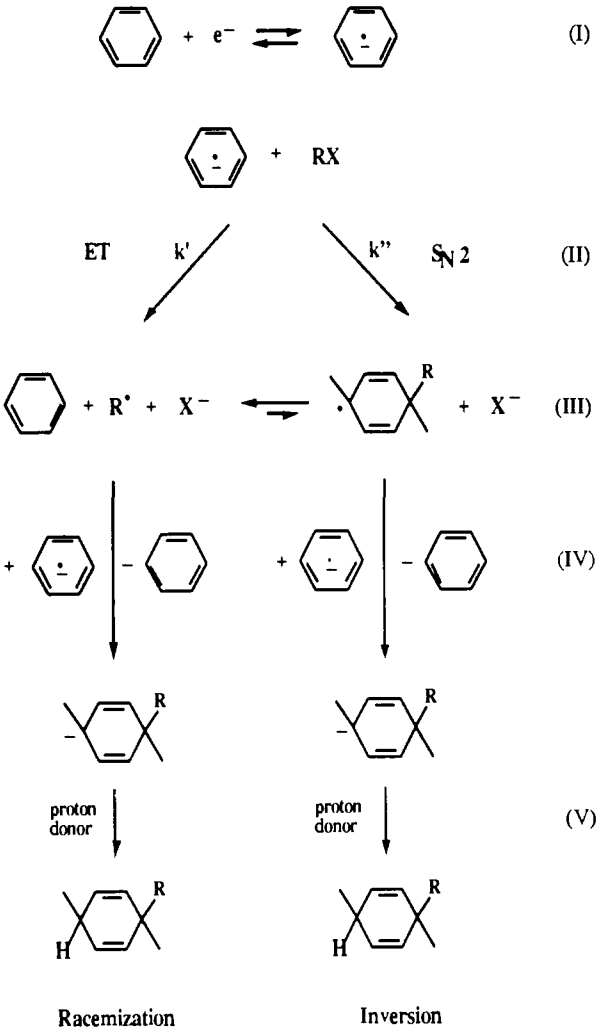

Symmetry Factor (Transfer Coefficient). If the activation–driving force relationship is quadratic as depicted in eq 1, the symmetry factor, α, (the transfer coefficient or Tafel slope of the electrochemist or the Brønsted slope of the homogeneous chemist) is expected to decrease upon raising the driving force in a linear way:

$$\alpha = \frac{\partial \Delta G^{\ddagger}}{\partial \Delta G^{\circ}} = \frac{1}{2}\left(1 + \frac{\Delta G^{\circ} - w_R + w_P}{4\Delta G_0^{\ddagger}}\right) \qquad (23)$$

If these predictions are correct, one would dispose of a useful experimental tool for analyzing mechanisms by utilizing the fact that a small α (i.e., distinctly below 0.5) would then indicate that the system reacts under a strong driving force and vice versa.

Testing of this particular aspect of electron-transfer dynamic model both for outer-sphere and dissociative electron transfers is easier in the electrochemical case than in the homogeneous case for several reasons. One is that the driving force may be changed in a precise and continuous way by varying simply the electrode potential, as opposed to the homogeneous case where changes in driving force require the use of a series of counter-reactants each

(15) (a) Lexa, D.; Savéant, J.-M.; Su, K. B.; Wang, D. L. *J. Am. Chem. Soc.* **1988**, *110*, 7617. (b) Daasbjerg, K.; Pedersen, S. U.; Lund, H. *Acta Chem. Scand.* **1991**, *24*, 470.

(16) (a) The above discussion seems to contrast recent ab-initio calculations concerning the reaction of the cation radical of ethane with hydrogen sulfide[16b] where the ET entropy was found smaller than the S_N2 entropy, this

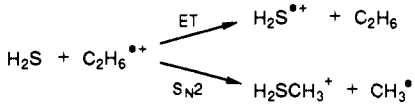

conclusion being inferred to be general in the ET–S_N2 dichotomy. The above reaction system is in fact rather different from that in the preceding discussion, since, here, an electron transfer not involving any bond breaking is compared to a reaction where concerted bond formation and bond breaking occur. The decrease in activation entropy upon passing from S_N2 to ET is then essentially related to the fact that the C–C bond is broken in the S_N2 reaction and not in the ET reaction. On the other hand, in the preceding dissociation, the C–X bond is broken in both reactions, and, in addition, a new bond is formed concertedly in the S_N2 case, leading to a decrease of the reaction entropy. (b) Cho, J. K.; Shaik, S. S. *J. Am. Chem. Soc.* **1991**, *113*, 9890. (c) The same trend, enhanced reactivity and decreased reaction entropy, is found in the reaction of reduced states of iron porphyrins with alkyl halides.[15a]

(17) Lexa, D.; Mispelter, J.; Savéant, J.-M. *J. Am. Chem. Soc.* **1981**, *103*, 6806.

(18) (a) Lund, T.; Lund, H. *Acta Chem. Scand. B* **1986**, *40*, 470. (b) Lund, T.; Lund, H. *Acta Chem. Scand. B* **1987**, *41*, 93. (c) Lund, T.; Lund, H. *Acta Chem. Scand. B* **1988**, *42*, 269. (d) Bordwell, F. G.; Hughes, D. L. *J. Org. Chem.* **1983**, *48*, 2206–2215. (e) Bordwell, F. G.; Bausch, M. J.; Wilson, C. A. *J. Am. Chem. Soc.* **1987**, *109*, 5465–5470. (f) Bordwell, F. G.; Wilson, C. A. *J. Am. Chem. Soc.* **1987**, *109*, 5470–5474. (g) Bordwell, F. G.; Harrelson, J. A., Jr. *J. Am. Chem. Soc.* **1987**, *109*, 8112–8113. (h) Bordwell, F. G.; Harrelson, J. A., Jr. *J. Am. Chem. Soc.* **1989**, *111*, 1052–1057.

of which introduces its own internal and external reorganization factors into the activation–driving force relationship together with those of the compound with which they exchange one electron. It is true that the work terms (double-layer correction) are more difficult to estimate in the electrochemical case, but they do not vary very much within the available range of driving forces.

In the case of outer-sphere electron transfer to aromatic molecules, the variation of α with the electrode potential (i.e., of the symmetry factor with the driving force) has received unambiguous experimental evidence and been found to be of the same order of magnitude as that predicted by the Hush–Marcus model (see ref 11 and references cited therein). In the case of dissociative electrochemical electron transfer to alkyl[8] and benzyl halides,[3] there is also evidence as discussed earlier that the transfer coefficient decreases upon raising the driving force.

Besides the variations of α with electrode potential that are necessarily small in accordance with eq 23, one is also striken by its small average value, ca. 0.3, i.e., distinctly smaller than 0.5 (the experimental values are actually slightly smaller than those predicted by the theory). There is so far no other models that could predict such low values resulting from another cause than the fact that the reduction potential is very negative to the standard potential of the $RX/R^{\bullet} + X^{-}$ couple.

Detection of a contingent variation of the symmetry factor of homogeneous electron-transfer reactions with the driving force is a much harder task for the reasons given above also taking account of the experimental uncertainty on rate measurements. There is not so far, even in the case of purely outer-sphere electron transfers, clear-cut direct evidence telling whether the symmetry factor does or does not vary with driving force. The situation is the same for the dissociative electron transfer involving aromatic anion radicals and alkyl halides in spite of recent claims that the log $k - E_{PQ}^{\circ}$ plots are linear rather than (slightly) parabolic and that the theory of dissociative electron transfer should be amended accordingly.[15b,19] The most interesting recent results in this connection concern the reduction of *t*-BuBr by an extended series of aromatic anion radicals in DMF,[15b] since, as discussed earlier, these electron donors behave in an outer-sphere fashion toward *t*-BuBr. The cyclic voltammetric data were extended toward lower rate constants by use of homogeneous kinetic techniques and toward larger rate constants by means of pulse radiolysis. Concerning this first extension, in view of the rather large scatter of the experimental points (when the dissociative electron transfer is slow, it is particularly difficult to avoid competing reactions of the aromatic anion radical with electrophilic and reducible impurities), there is no real gain in the possibility of discriminating between the linear and slightly parabolic behavior. For what regards the pulse radiolysis experiments, it is difficult, in the absence of experimental details, to evaluate the contingent sources of uncertainties and systematic errors. From another pulse radiolytic study,[19] it appears that, for the same aromatic anion radical, the rate constant appears to be larger than the electrochemical rate constant (by a factor of about 3). There might indeed by a systematic difference between the rate constants gained by one or the other methods arising from different experimental conditions (for example, the pulse radiolytic experiments are usually carried out in the absence of supporting electrolyte and at much lower concentrations than in electrochemistry). On the other hand, rate constants close to the diffusion limit do not allow a precise determination of the activation controlled rate parameters. Taking these uncertainties into account, it appears that the available data neither disprove nor prove for the time being the slight variation of α with the driving force expected from the theory. What is however clear in these experiments is that the average value of α one can derive from a straight-line fitting, 0.4, is clearly below 0.5, which falls in line with what is expected from the theory, taking account of the fact that most of the experimental points are located at potentials negative to the standard potential of the $RX/R^{\bullet} + X^{-}$ couple.

Adding to this that the electrochemical α is smaller than the average homogeneous α, in agreement with the larger driving force in the electrochemical case, it may be concluded that the quadratic model correctly predicts the magnitude of the symmetric factor, particularly the expectation that it should be distinctly smaller than 0.5 under large driving forces.

Conclusions

Improvement of the theory of dissociative electron transfer necessitates the taking into account of the effect of solvent relaxation and resonance energies at the transition in the description of the reaction dynamics. Uncertainties in the determination of these factors render difficult an absolute estimation of the preexponential factors that would allow the testing of the theory with available experimental data. The estimation of the solvent reorganization energy is also subject to large uncertainties. A strategy that allows one to circumvent these difficulties consists of estimating an appropriate combination of these various factors from available experimental data pertaining to outer-sphere electron-transfer reactions in which solvent reorganization is the main factor of activation and transferring this information into the treatment of the rate data for dissociative electron-transfer reactions in the same solvent.

Application of this strategy to the electrochemical and homogeneous reduction of alkyl halides in DMF, making use of previous data concerning an extended series of aromatic molecules in the same solvent, proved successful. In the electrochemical case, there is a good agreement between the theoretical and experimental values of the intrinsic barrier for the whole set of butyl iodides and bromides and for benzyl bromide and chloride.

In the homogeneous reduction of alkyl halides by aromatic anion radicals, there is also a good agreement between theoretical predictions and experiment in the case of tertiary butyl and benzyl halides. With secondary and primary halides, the reaction is systematically faster than predicted by the theory. These observations point to the conclusion that while aromatic anion radicals react in an outer-sphere manner with tertiary halides, the reaction has an S_N2 character, involving small bonded interactions in the transition state, in the case of primary and secondary halides, in accord with previous stereochemical results and with the observation that the reaction entropy decreases from tertiary to secondary and primary halides.

Registry No. BuI, 542-69-8; *s*-BuI, 513-48-4; *t*-BuI, 558-17-8; BuBr, 109-65-9; *s*-BuBr, 78-76-2; *t*-BuBr, 507-19-7; BuCl, 109-69-3; *s*-BuCl, 78-86-4; *t*-BuCl, 507-20-0; $PhCH_2Cl$, 100-44-7; $PhCH(CH_3)Cl$, 672-65-1; $PhC(CH_3)(CH_2CH_3)Cl$, 67765-94-0; $PhCH_2Br$, 100-39-0.

(19) Grimshaw, J.; Langan, J. R.; Salmon, G. A. *J. Chem. Soc., Chem. Commun.* **1988**, 1115.